Fluid inclusions in salt from the Rayburn and Vacherie domes, Louisiana

Edwin Roedder and H.E. Belkin

U.S. Geological Survey Open File Report

Abstract

Core samples from the Rayburn and Vacherie salt domes in Louisiana were examined for fluid inclusions, in connection with the possible use of such domes for nuclear waste storage sites. Three types of fluid inclusions were found, brine, compressed gas, and oil (in decreasing volume percent abundance). The total amount of such fluids is small, certainly < 0.1 vol. % and probably in the range 0.01 to 0.001 volume %, but the inclusions are highly erratic in distribution. Unlike many bedded salt deposits, the brine inclusions in this salt contain fluids that are not far from simple NaCl-H_2O solutions, with very little of other ions. One of three possible explanations for such fluids is that fresh water penetrated the salt at some unknown time in the past and was trapped; if such entry of fresh water has occurred in the past, it might also occur again in the future.

Samples studied

In 1978 one of us (ER) selected eight samples of core from the Rayburn dome, Bienville Parish, LA (D.O.E.-C.F.I. no. 1 core), and ten from the Vacherie dome, Webster Parish, LA (D.O.E. Smith no. 1 core), from the core storage rooms at the Louisiana State University Institute for Environmental Studies. The samples (see Table 1) were selected in part to be representative of the various lithologies visible in the cores, based on L.S.U. studies, and in part to obtain material most likely to contain useful fluid inclusions, based on visual inspection and past experience.

In addition to the above, one sample of granular salt from the upper level of the mine in Week's dome, ~600' below surface, was also obtained.

Procedures used

Petrographic examination

All samples were examined under the microscope by normal petrographic techniques, in cleavage fragments and/or doubly polished plates, prepared with suitable care to avoid loss or damage to inclusions. Inclusion occurrence, size, abundance, and nature were noted, and then suitable inclusions in appropriately-sized portions were removed for study by the following methods.

Freezing stage

In this microscope stage the sample is cooled, either with a flow of refrigerated acetone (Roedder, 1962) or nitrogen (from evaporation of liquid nitrogen; Poty et al., 1976), and the phase changes on cooling and on reheating are watched. Several specific temperatures are normally noted: the freezing temperature, the first melting temperature, and the final melting temperature. The first of these is of relatively minor significance, since it represents a non-equilibrium phase change. Nucleation and crystallization of inclusion fluids normally takes place only after considerable supercooling. The amount of supercooling found provides at best only a crude indication of the effectiveness of any nucleation agents that may be present in the fluids. The first melting temperature is the temperature during warming at which a completely frozen inclusion, consisting solely of solid salts and ice (and hence nearly opaque), develops enough liquid phase to wet the interfaces between the crystals and become translucent. Although inexact (it can seldom be

repeated to better than one or two degrees), it provides a measure of the eutectic melting temperature of the chemical system represented by the inclusion fluid. The final melting temperature is the temperature at which the last solid phase (other than the host crystal walls) disappears on warming. Metastability due to failure to nucleate a phase is avoided by approaching only from below, i.e., by obtaining the temperature of disappearance of the solid phase. This temperature, and the composition of the last phase to melt, when compared with appropriate phase diagrams, place some limits on the composition of the fluid in the inclusion.

Heating stage

In this microscope stage the sample is heated while observing the phase changes within the inclusion. The most common phase change is that of expansion of the liquid phase causing elimination of the shrinkage vapor bubble that is generally present at room temperature.

Pressure determination

Two different methods were used to determine the gas pressure in the inclusions, the crushing stage, and the water dissolution technique. In the crushing microscope stage the sample is compressed uniaxially, parallel with the microscope optic axis, while immersed in a liquid of matching index of refraction (Roedder, 1970). When a fracture contacts an aqueous inclusion, two possible behaviors may be observed. If the vapor bubble in the inclusion was from shrinkage, it contains only a few millimeters of water vapor pressure, and will collapse instantly. If, however, the bubble contains gas under a pressure greater than atmospheric, it will expand against the atmosphere when exposed by the intersecting fracture.

The water dissolution technique provides the same type of data. In

this, the sample is dissolved in water under the microscope, while watching a given inclusion. If the advancing solution front is correctly oriented to the line of sight at the time of its intersection with the inclusion, the same types of behavior can be observed as occur when a crack intersects the inclusion. In either method, the measurement of the volume of the bubble before and after permits an estimate of the volume expansion. Such a measurement is probably only accurate to $\pm$ 10% at best.

Thermal gradient migration runs

In this test, a rectangular block of salt, 1x1 cm in cross section, and containing suitable inclusions, is cut out and the position of the inclusions photographed against a series of fiducial marks. The block is then placed in a 1x1 cm slot in the center of a cylindrical segmented Teflon block (see Figure 1), in tandem with other similar salt blocks, with appropriately-placed thermocouple junctions, and the whole assembly is placed in a thermal gradient furnace with appropriate controls for both ambient temperature and superimposed gradient (Roedder and Belkin, 1979b). The gradient is established and maintained along the length of the cylinder, perpendicular to the section shown in Fig. 1. The samples are heated to the desired temperature gradient and ambient temperature slowly to avoid thermal stress, and then held constant under these conditions for some days. After slow cooling, the samples are rephotographed and movement of the inclusions relative to the fiducial marks is measured.

Results

The results for samples from the two domes, Vacherie and Rayburn, were sufficiently similar that the following discussion is generally applicable to both groups of samples. This lack of differences could be merely a result of the limited number of samples and inclusions tested.

Petrographic examination

Detailed petrographic descriptions of these cores are being made by the group at Louisiana State University, so only those features of particular pertinence to fluid inclusion study will be mentioned here. Table 1 lists the general nature of the samples, and since these samples were taken in part to cover the range of lithologies, they probably are representative of the range. Three types of fluid inclusions were found, brine, compressed gas, and oil; brine was by far the most abundant in volume by a considerable margin, but compressed gas inclusions were the most numerous. The total volume percent of fluid inclusions evident in these samples is low in all. The distribution is too erratic to permit a good estimate from the available sampling, but it would seem to fall generally somewhere in the range of 0.01 to 0.001 vol. %. Only very small portions of the samples examined would approach 0.1 vol. %. Some of the large single-crystal samples were essentially free of visible fluid inclusions. All samples contained at least a few anhydrite crystals, and some contained anhydrite-rich bands.

Brine inclusions - Some brine inclusions occur as isolated relatively large ($\leq$1mm) inclusions in salt, with or without an included anhydrite crystal (Figs. 2-5). As is generally true in salt, small liquid inclusions without anhydrite are equant negative cubes, and large free inclusions are more irregular (e.g., Fig. 3). Most brine was found, however, as fillets between adjacent anhydrite crystals, where it is difficult to recognize without strongly convergent illumination (Figs. 6 & 7). Under normal microscope illumination, such fluid inclusions disappear into the black borders from total reflection at the anhydrite-salt and salt-brine interfaces. This common occurrence of the brine inclusions suggests a

preferential wetting, but other brine inclusions, even in anhydrite-rich salt, are not in contact with any anhydrite crystal (e.g., Fig.5a). Some inclusions appear to be stretched out between two anhydrite crystals (Figs. 8 & 9); it is possible that such features formed as a result of two adjacent anhydrite crystals, with a fillet of brine between, being pulled apart by flowage of the host salt. As these inclusions are in a large single crystal of salt, presumably there was a subsequent recrystallization. (Deformation and recrystallization have apparently been extensive and repeated processes in these samples, and some large, clear single crystals of salt now have strongly curved cleavage planes, with a radius of curvature $\gtrsim$ 30cm.).

All but the smallest brine inclusions contain a vapor bubble of ~1 vol. % (Table 2). Several inclusions were found with dark or opaque specks adhering to the bubble surface (e.g., Fig. 2); these might well be organic matter (Roedder, 1972).

One of the most important questions in most fluid inclusion work is that of the origin of the inclusions studied: primary, pseudosecondary, or secondary (see Table III in Roedder, 1976). Unfortunately, the origin of most of the inclusions in these samples is obscure at best. Many of the samples contain planes of obvious secondary inclusions, outlining former cubic cleavage fractures (i.e., parallel to (100)). Other similar planes of secondary inclusions are found outlining fractures that are close but not necessarily exactly parallel to the dodecahedron ((110); see Fig. 10), along which slip has apparently taken place. Such inclusions must postdate the host salt. But the large, isolated inclusions within visibly undeformed salt, on which most of the work was done, may represent

fluids from almost any part of the history of the salt prior to the last recrystallization. Thus they could represent seawater, trapped within the original salt (as in many bedded salts; Roedder & Belkin, 1979a), which has coalesced during flowage. They could equally well represent near-surface groundwaters which flowed into fractures in the moving salt dome, and were trapped by rehealing of the host crystal. Inclusions in salt can move and recrystallize so readily (Roedder amd Belkin, 1979b) that the present shape and occurrence of such inclusions provide no real clues.

Compressed gas inclusions - At least a few tiny dark specks (generally ~1-2μm) are visible at the contact between most included anhydrite crystals and the host salt (Figs. 6 & 7). Where these are large enough, they are seen to be transparent colorless blebs with no features visible internally. Most of the larger such blebs appear to be arranged in some semiregular fashion, presumably in response to minimum surface energy requirements against salt, anhydrite, or both (Figs. 11 & 12). On pressure determination (see below) these are found to consist of gases under high pressure. Similar high pressure inclusions are found around anhydrite crystals in the "popping salt" of the Winnfield salt dome in Winn Parish, LA (Fig. 13).

Oil inclusions - Some of the larger inclusions on the surface of anhydrite crystals are strongly colored, generally in browns (Fig. 14). These are assumed to be oil inclusions, solely on the basis of the color and the odor of petroleum upon breaking some of these samples. Some planes of secondary inclusions (e.g., Fig. 15) contained three fluids: a host fluid (brine), a tiny bubble of gas with a very much lower index of refraction

than the brine, and another bleb of fluid very obviously higher in index than the brine. This last is probably an oil that was present in dispersed droplets in the fluid surrounding this crystal at the time the crack formed. The volume percent of oil varies widely from one inclusion to another (Fig. 16).

Freezing stage results

The freezing temperatures of the brine inclusions ranged from a maximum of -67°C to a minimum of -102°C, the first melting temperatures were mostly -21°C to -25°C, and the final melting temperatures were ~+1.0°C (see Table 2). The difference between the freezing temperature (i.e., metastable supercooling) and the final melting temperature (i.e., stable equilibrium) represents the amount of supercooling these inclusions underwent before finally nucleating ice and salts. Most fluid inclusions in most minerals exhibit similar supercooling. It tells us only that these are very clean fluids, free from the numerous submicroscopic freezing nuclei so commonly present in rapidly moving surface waters. No freezing studies were made of the gas or oil inclusions.

The first melting temperatures given in Table 2 range from -21.1°C to -33.1°C and average -23.7°C. These are the highest values obtained in several runs on each inclusion. The differences between highest and lowest values were not large, averaging 2.4°C. The rationale for choosing the highest value is that metastable assemblages melt at lower temperatures than the stable ones. Thus in the pure system $NaCl-H_2O$, the stable assemblage at first melting should be hydrohalite ($NaCl \cdot 2H_2O$)-ice-solution at -21.1°C, but as hydrohalite is sluggish to form, the metastable eutectic between NaCl and ice at ~-28°C (Roedder, 1962) is relatively easy to

observe. The significance of the first melting temperatures found is that these inclusions must contain fluids that are close to pure NaCl-H_2O mixtures, since all other salts added to NaCl-H_2O mixtures lower the eutectic below the -21.1°C minimum in the pure system. Only small amounts of other salts are needed to make the change from -21.1°C to the average found here, -23.7°C, or even to the lowest temperature, -33.1°C. In contrast, some inclusions in halite from the Lower Salado bedded salt of the WIPP site near Carlsbad, New Mexico had first melting temperatures as low as -56°C (Roedder and Belkin, 1979a).

The final melting temperatures found (Table 2) are a further verification of the probability that these inclusions consist of essentially NaCl and H_2O. In the pure system NaCl-H_2O, an inclusion of pure water, saturated with NaCl, in an NaCl host crystal, should, at equilibrium, consist solely of solid hydrohalite at all temperatures below +0.10°C (Roedder, 1962). On warming to this temperature, this compound should melt completely and incongruently to form NaCl (precipitated on the walls) plus liquid. The fact that these inclusions showed at least some liquid over the range between their first melting temperature and their final melting temperature is the result of the presence of some (at present unknown) materials other than NaCl and H_2O. The last crystal to melt in these inclusions had an index of refraction and birefringence suggesting hydrohalite; its presence in these inclusions at temperatures as much as 2.4°C above the known incongruent melting point of the pure compound (+0.10°C) is probably a result of the well-known and remarkable sluggishness of this compound to melt. Adams and Gibson (1930) found that crystals of this compound required over an hour to melt, when held at +4°C, almost 3°C over their equilibrium melting temperature.

Heating stage results

As might be expected from the very small vapor bubbles in these brine inclusions, averaging 1.0% (Table 2 and Figs. 2-5), the homogenization temperatures are low, ranging from 48 to 111°C, and averaging 72°C (Table 2). Some inclusions that appear to have a larger bubble, e.g., Figs. 2 and 4, are misleading because they are thick in the third dimension. There is no apparent correlation between the homogenization temperatures and the volume percent vapor bubble (Table 2), although there should be. We suspect that this results from the rather large uncertainties in measuring the volume of irregular inclusions (particularly in estimating the third dimension). Some inclusions have maintained a metastable, "stretched liquid" state, under negative pressure, from failure to nucleate a vapor bubble (Roedder, 1967). On cooling below room temperature these formed a bubble that persisted on warming back to room temperature.

We cannot readily relate these homogenization temperatures to formation temperatures. In addition to the problem of estimating a pressure correction (were these inclusions formed at the time of the original deep burial (~10-12km), during the salt dome ascent, or in essentially the present sample locations, after dome stabilization?), is almost certain that some permanent deformation of the inclusion walls from internal pressure can be expected for any inclusions in salt that have been moved from a higher to a lower external pressure. The expansion of fluid inclusions in salt from internal pressure on overheating for days (or even minutes) in the laboratory (Roedder and Belkin, 1979a) proves the plasticity of salt under these conditions, and hence the present homogenization temperatures might only represent an approach to equilibrium volume relations at the P and T of the sample site[1/]. As an example, one rather large inclusion from Rayburn (volume

1/ Down-hole temperatures of $\leq$ 72°C were encountered in the Vacherie boring.

$2.2 \times 10^{7} \mu m^3$, i.e., $2.2 \times 10^{-5} cm^3$), that originally had a small bubble (0.1%) never did homogenize. The bubble was larger at 230°C than at room temperature, due to this permanent deformation or stretching of the walls. This inclusion contained gas under pressure (see next section). The fact that the homogenization temperatures show a rough inverse correlation with sample depth may result from incomplete equilibration with the ambient pressure during dome uplift, modified by the effects of local nonhydrostatic pressures, gases under pressure, or other factors.

Pressure determinations

A total of >100 fluid inclusions and ~30 solid inclusions were tested for gas pressure, mainly by the water dissolution technique. The results were essentially similar for samples from Vacherie and Rayburn. Approximately 95% of those brine inclusions that had an initial bubble evolved a larger bubble, i.e., they contained gas under pressure > 1 atm. (Figs. 17-22). The amount of expansion ranged from 1.4 to ~4000 times the original bubble volume, but with no recognizable systematic relation to any observed parameter. If the volume increase is solely from expansion of gas originally in the bubble, a 2-fold expansion, e.g., would indicate a pressure of approximately two atmospheres in the inclusion. As even liquified gases such as CO_2 expand only ~350-fold on converting to a gas, the 4000-fold expansion found for one inclusion from Vacherie that was presumed to be brine can only signify that it originally contained not a water solution, but a volatile liquid, such as liquified hydrocarbon gases under pressure, plus a very small vapor bubble. In opening, not only did the vapor bubble expand, but the entire mass of liquid changed to gas. The vapor pressure of this liquid must have been only slightly

> 1 atm, since it did not flash into vapor, but took several seconds, presumably as the heat of vaporization diffused in from the surroundings.

The bubble in a few inclusions collapsed completely, indicating the absence of noncondensable gases in these bubbles. This test is exceedingly sensitive, as only 10^9 molecules (i.e., $\sim 10^{-14}$ g) of such gas are needed to make a readily visible bubble several micrometers in diameter (Roedder, 1970). Other inclusions had no initial bubble; on pressure release, each of these nucleated one, which expanded to a size range similar to those observed above.

When a solid anhydrite crystal was intersected by a fracture or a solution front, a bubble always evolved (Figs. 23-24). Presumably this represents the expansion of the minute gas films and inclusions commonly observed at the interface between anhydrite and salt, as seen in Figs. 11-12, although gas bubbles formed from some anhydrite crystals that had no visible gas inclusions. Presumably a film of gas under pressure, too thin to be visible, must be present at the interface. As the volume of these minute compressed (and probably liquified) gas inclusions can be determined only very roughly, the pressure in them can only be estimated. The large expansions observed suggest pressures in the range of hundreds of atmospheres. Inclusions containing mainly CO_2 or CH_4 under high pressure are probably responsible for some of the large spontaneous and disastrous mine "blowouts" of thousands of tons of salt at other salt domes in Louisiana and elsewhere (Fig. 13; Roedder, 1972, p. JJ43). A significant amount of gas under pressure was encountered in the Vacherie drilling, and gases, containing traces of H_2S, were found in the cap rocks of both domes.

Thermal migration run

A thermal migration run of 180 hours duration was made with a 157°C ambient temperature and a gradient of $1.5°C \cdot cm^{-1}$. Sixteen inclusions were measured, with volumes in the range of 2.0×10^4 to $2.6 \times 10^6 \mu m^3$ All migrated up the gradient, at rates that were directly but only approximately proportional to their initial volume. The rates of migration were in the same range as those obtained for equivalent-sized inclusions in Salado salt from the WIPP salt in the same experiment, i.e., about $0.4\ cm \cdot yr^{-1}$ for inclusions of $\sim 10^6 \mu m^3$ volume. The similarity of these values is of interest, as the lower solubility of NaCl in the strong bitterns present in the Salado salt would be expected to yield significantly lower rates of migration (Roedder and Belkin, 1979b).

Significance

Three aspects of this work are significant to the problems of the possible use of such salt domes as nuclear waste storage sites in several ways. First, the amount of water found in inclusions in this salt is very low, one or more orders of magnitude lower than that found in several bedded salts (Roedder, 1963; Roedder and Belkin, 1979a). It is not known if the amount of water found is representative of the material in the dome, but the amounts actually seen in fluid inclusions must represent a minimum value for that which is in situ in the dome. Whether this amount of water is adequate to cause engineering problems in a nuclear waste storage site has not been addressed by this study.

Second, the freezing stage studies show that except for some liquid and gaseous hydrocarbons, the fluids in these inclusions are essentially just saturated $NaCl-H_2O$ brines, with very little of other ions such as

Ca, Mg, and K that are commonly found in large amounts in the inclusions of most bedded salts (Roedder, 1963; 1972; Roedder & Belkin, 1979a). Fluids containing these other ions, whether they be residual brines from the original evaporation of sea water, or newly-formed brines from diagenetic changes among the several minerals present in the bed, were presumably "kneaded" out of these salt samples during flowage. (Brines high in calcium do occur in some Louisiana dome salts.) The most significant feature, however, is not the lack of such multi-ion fluids, but the fact that there are essentially pure $NaCl-H_2O$ fluids present. Nearly pure $NaCl-H_2O$ fluid in a salt bed can have three possible origins: 1) It can be sea water trapped in the first-formed salt crystals, before evaporation and crystallization caused much buildup of other ions. 2) It can be water evolved by the dehydration of clay minerals or the conversion of other phases such as gypsum to anhydrite during diagenesis. 3) It can be fresh water which has penetrated the salt at some unknown time in the past and been trapped.

The third possibility has the greatest potential importance to the possible use of these domes for nuclear waste storage. At the depth from which these originally bedded salts have flowed to form these domes (~10-12km), the fluids in the pores of the surrounding sediments were almost certainly highly saline formation waters, with significant ions other than Na and Cl. But during the rise to the surface, the salt dome must have penetrated aquifers with essentially fresh water. If fracturing occurred during this rise, or subsequently (and we have no knowledge of the age of these inclusions), fresh waters could enter the salt and become trapped. The corollary is that if this happened in the past, it might also happen in the future.

Acknowledgement

The authors are indebted to Drs. J. Martinez and Ron Wilcox of the Louisiana State University Institute for Environmental Studies for help in selection of suitable samples, and to Marc Wouters for assistance in the laboratory.

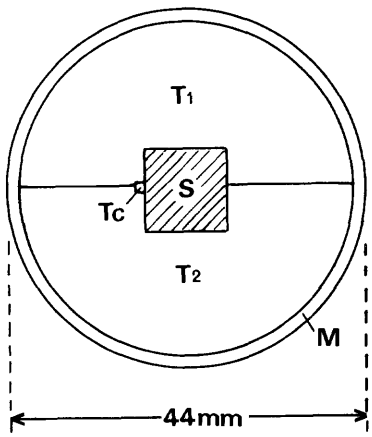

Fig. 1. Cross section of thermal migration experiment sample holder. The sample (S) consists of a 1x1 cm block of salt, in a closely-fitting slot between two hemicylindrical Teflon blocks (T_1 and T_2), 41 mm in diameter, which fit closely into a closed-end Inconel tube (M) of 1.5-mm wall thickness and 18 cm length. Thermocouples (T_c) are placed along the salt at known positions.

2

3

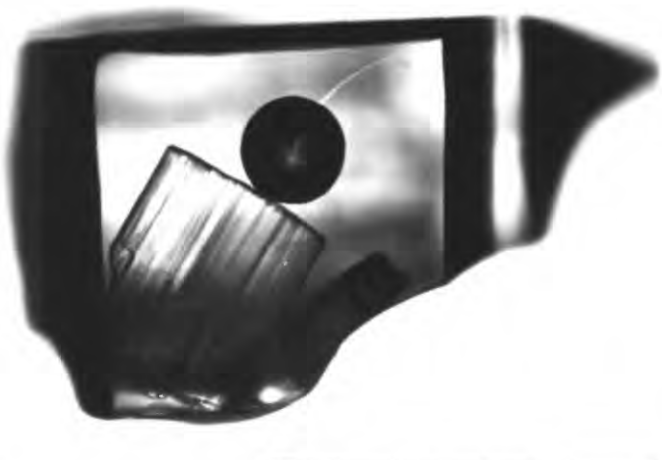

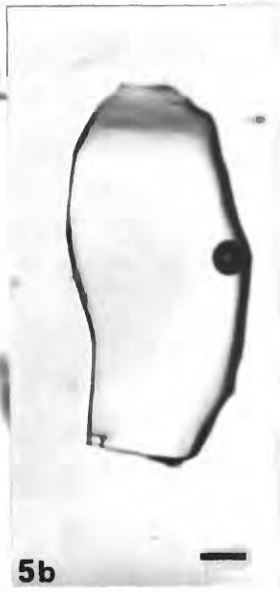

4

5a

5b

Fig. 2 Partly faceted brine inclusion, with small particles of organic matter(?) sticking to surface of bubble (arrows). Temperatures of homogenization 110°C, first melting -22.5°C, final melting +1.9°C. Vacherie 1067.7'. Scale bar = 100 μm.

Fig. 3 Large irregular brine inclusion with very small bubble (arrow). Rayburn 1784.5'. Scale bar = 1mm.

Fig. 4 Large brine inclusion with included anhydrite crystal. Vacherie 1067.7'. Scale bar = 1mm.

Fig. 5a Large brine inclusion which, although it is in anhydrite-rich salt, has no contact with anhydrite. Rayburn 1784.5'. Scale bar = 100 μm.

Fig. 5b Large irregular brine inclusion with small bubble. Vacherie 1067.7'. Scale bar = 100 μm.

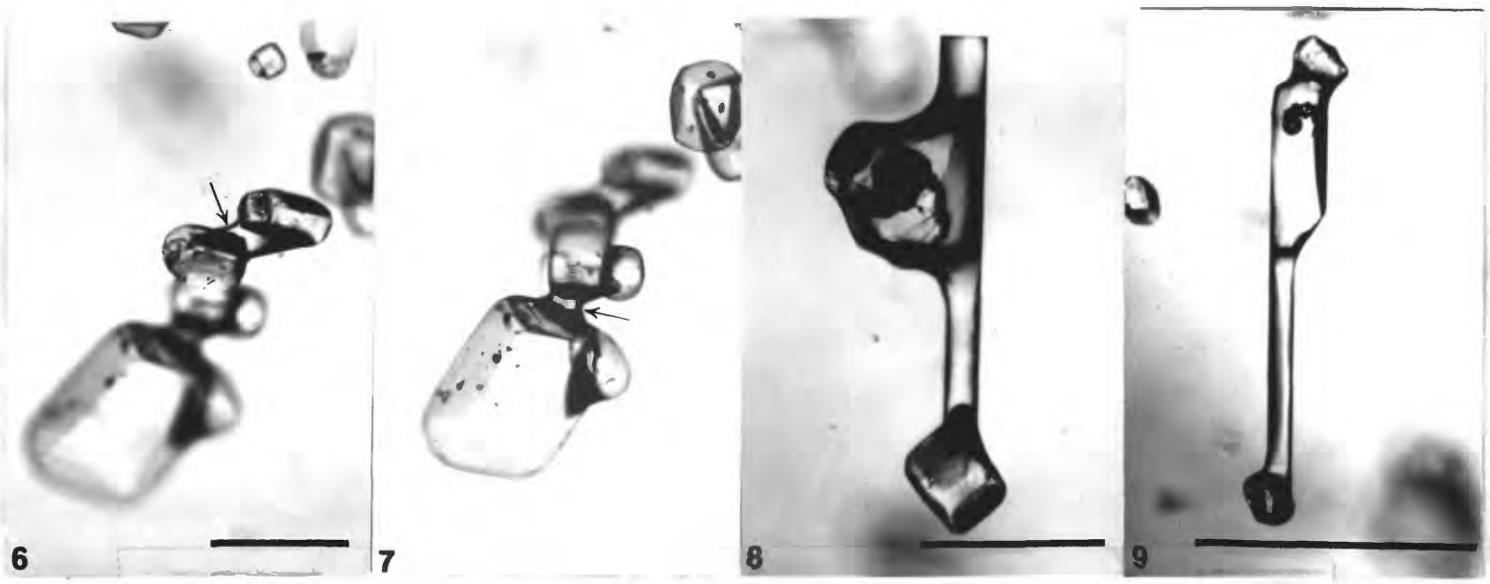

Fig. 6 Group of anhydrite crystals with fillet of adhering brine (arrow) taken in strongly convergent light. Rayburn 1784.5'. Scale bar = 500 μm.

Fig. 7 Same group of anhydrite crystals as Fig. 6, at different level of focus, showing another fillet of brine (arrow), in strongly convergent light. In normal collimated microscope lighting, these fillets are hidden in broad black shadows.

Fig. 8 Semi-negative crystal brine inclusion between several anhydrite crystals. Rayburn 1410'. Scale bar = 500 μm

Fig. 9 Inclusion similar to that in Fig. 8 and near to it in same sample. Several such inclusions were all parallel, suggesting direction of stretching or shearing of host salt. Scale bar= 1 mm.

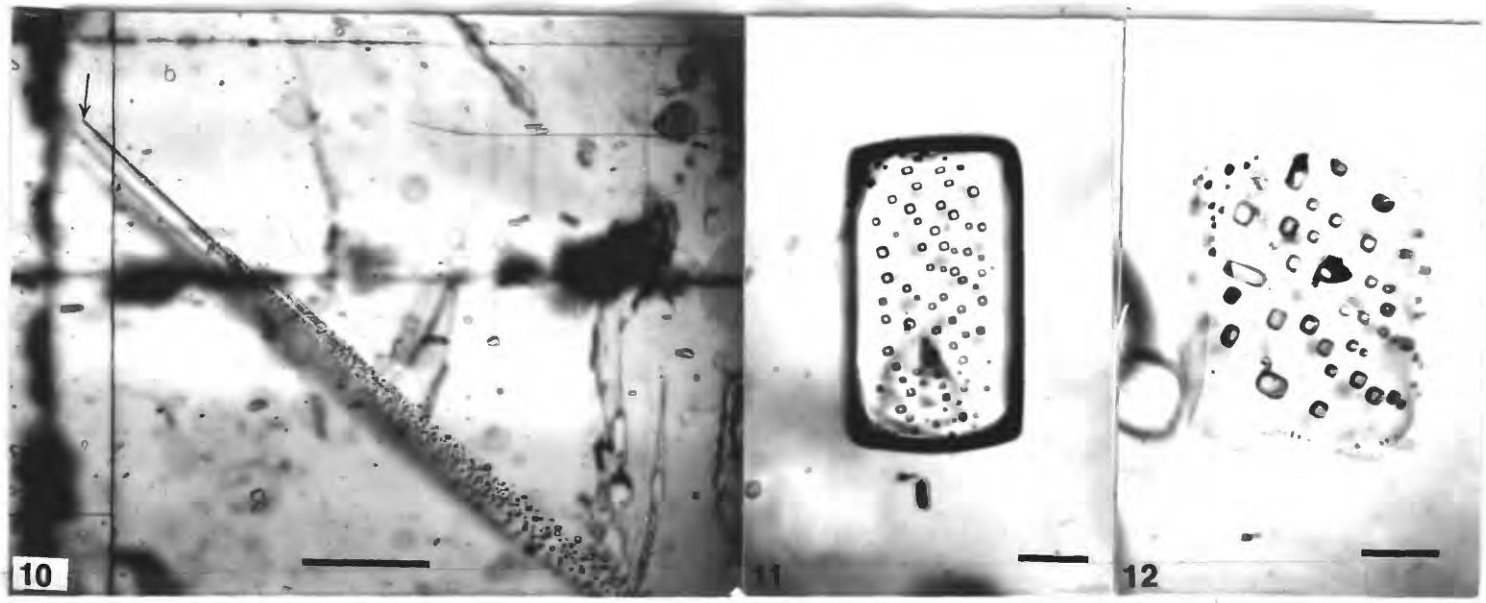

Fig. 10 Crystal of salt with cubic cleavage directions vertical, horizontal, and parallel with plane of the picture, with a group of planes of secondary inclusions arranged parallel to the dodecahedron (110), presumably from slippage. The individual members are visible only at the end of the group (arrow), where the original cracks pinch out. Week's dome, 600'. Scale bar = 1 mm.

Figs. 11 & 12 Group of semi-oriented inclusions of compressed organic(?) gas at interface between anhydrite crystal and host salt. Rayburn 1784.5'. Scale bars = 100 μm.

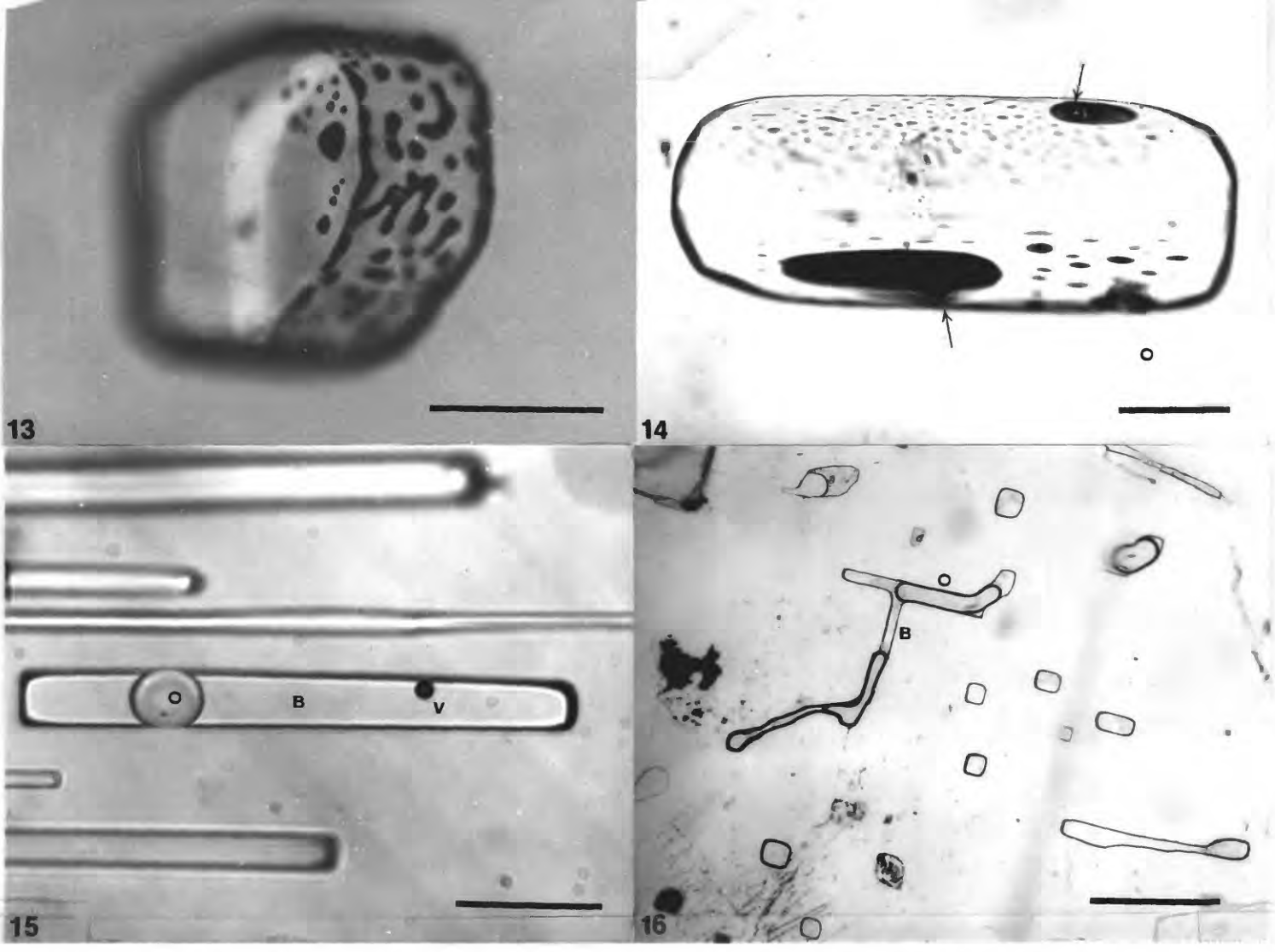

Fig. 13 Anhydrite crystal in salt from Winnfield dome, Winn Parish, LA, with compressed gas inclusions (dark) at interface. Scale bar = 100 μm.

Fig. 14 Inclusions of dark brown fluid, presumably oil, with vapor bubbles, (arrows) on surface of anhydrite crystal in salt. Rayburn 1784.5'. Scale bar = 100 μm.

Fig. 15 Plane of secondary inclusions in salt with tiny dark vapor bubble (V) and immiscible droplet of oil (O) in brine (B). Week's dome, 600'. Scale bar = 100 μm.

Fig. 16 Plane of secondary inclusions in salt consisting of brine (B) and oil (O). Vacherie 1067.7'. Scale bar = 500 μm.

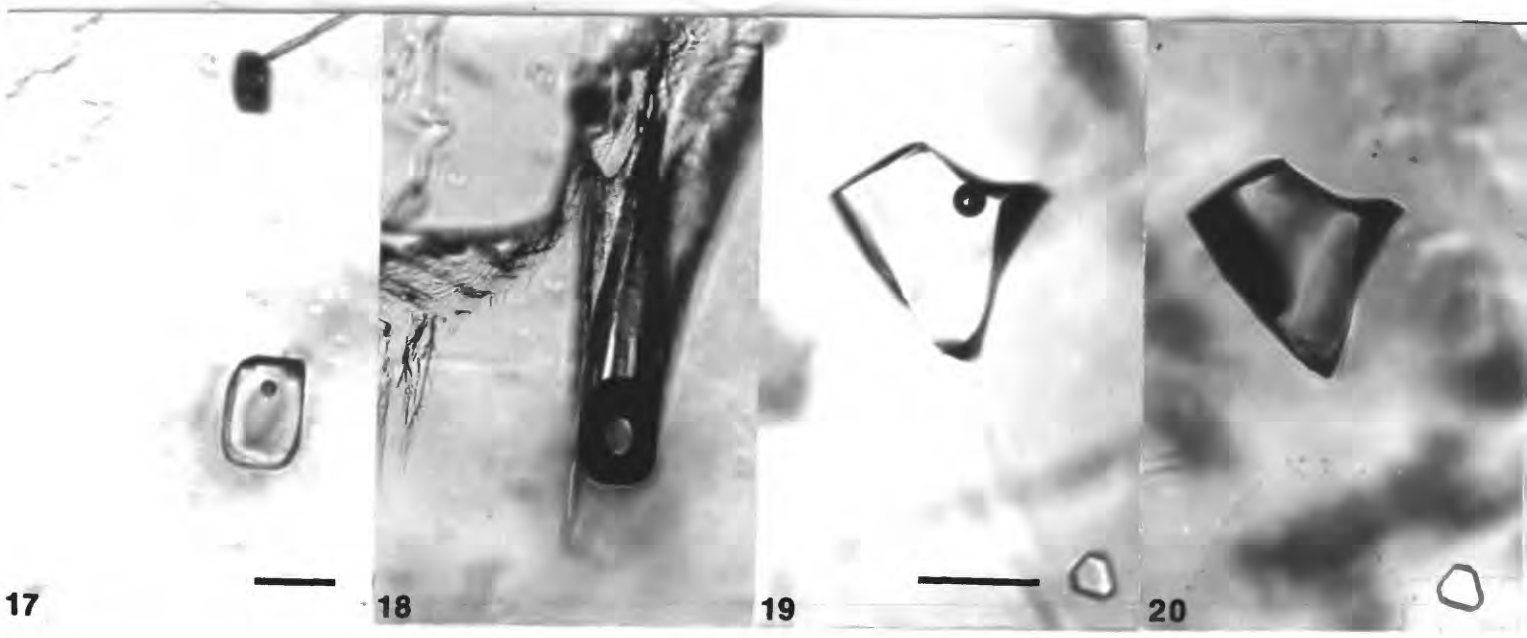

Fig. 17 Inclusion with high pressure gas bubble on crushing stage before crushing. Vacherie 1432.5'. Scale bar = 100 μm.

Fig. 18 Same field as Fig. 17, after fracture intersected inclusion; the gas bubble has expanded to fill the inclusion, pushing out the brine, Total expansion 238-fold.

Fig. 19 Inclusion with high pressure gas before solution front (above and approximately parallel with plane of photograph) intersects it. Vacherie 1432.5'. Scale bar = 100 μm.

Fig. 20 Same field as Fig. 19 after intersection of solution front with inclusion. All brine has been pushed out and bubble has expanded to fill the inclusion. Total expansion 342-fold.

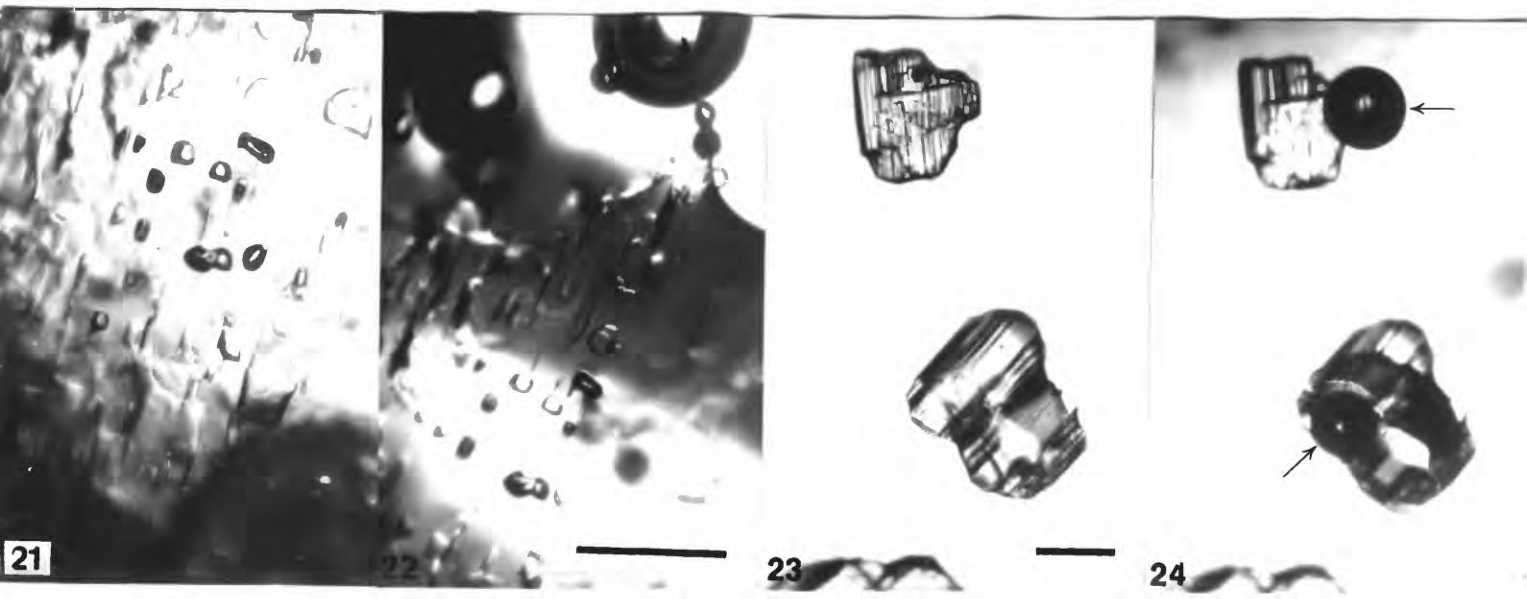

Fig. 21 Plane of secondary high pressure gas inclusions before solution front intersects. Rayburn 168-170'.

Fig. 22 Approximately same field as Fig. 21, after sloping solution front has contacted some of the secondary high pressure gas inclusions. Scale bar = 100 μm.

Fig. 23 Two anhydrite crystals in salt. The solution front is advancing parallel to plane of the photograph but has not yet intersected the inclusions. Scale bar = 100 μm.

Fig. 24 Same field as Fig. 23 after solution front contacts these two crystals. Note large gas bubbles (arrows) formed from almost invisible high pressure gas inclusions.

Table 1. Salt samples examined

Rayburn Dome

Core Box #	Notes	Depth (ft.)
4-1	Dark anhydr.-bearing salt	168-170
8-5	Granular salt	384-385
20-15	Equigranular salt	1112
	Coarse single crystal salt	1410
	Coarse single crystal salt	1450
32-6	Coarse single crystal salt ("paleo-spirit level" sample)	1781.4
32-7	Coarse single crystal salt; photographed	1784.5
35-14	Representative coarse single crystal salt	1971.

Vacherie Dome

1-6	Celestite crystals (from cap)	561
8-10	Coarse and fine salt	885
11-15	Coarse single crystal salt	1067.7
15-bottom	Granular salt	1325-1330
17-18	Coarse single crystal salt (curved cleavage) with thin boudinaged anhyd. seams	1432.5
20-22	"Megacrystalline salt"; slight odor of H_2S on breaking	1625.5 (base)
27-6	"Fine-grained", granular salt	1933-1935
29-20	"Megacrystalline" salt	2083.0 (top)
39-24	Granular salt	2655-57
51-15	Coarse single-crystal salt adjacent to anhydr. layer; some odor of oil	3222.5

Table 2. Petrographic, heating stage, and freezing stage data on inclusions in halite from salt domes.

Depth (ft)	Inclusion origin[1]	Vapor bubble 5/ (vol. %)	Total volume 5/ (μm^3)	Temperature (°C) 2/ First melting	Final melting	Homogenization
			RAYBURN dome			
168-170	P	0.2	1.0×10^5	-25.4	+0.8, +0.9, +1.1	76,74
"	P	0.5	1.9×10^7	--	---	--
"	S	1.4	1.4×10^5	-23.2	+2.4, +2.5	85,84
1410	P	3.2	1.3×10^7	-21.1	+0.2, +0.3	100,100
"	P	1.1	9.7×10^6	-22.6	+0.6, +0.1	--
"	P	1.0	4.5×10^7	--	--	>96 4/
1784.5	P	1.3	1.1×10^5	-22.5	0.0	54
"	P	0.5	8.0×10^5	-24.0	-1.6, -1.4	54
"	P	0.8	1.5×10^5	-22.0	0.0	51
"	P	0.7	3.7×10^5	-23.0	0.0, -1.4	57.5
"	P	0.1	7.6×10^5	-23.0	0.0, -1.4	56
"	P	0.7	5.9×10^5	-24.0	0.0, -1.4	54
"	P	0.7	2.1×10^5	-24.0	0.0, -1.5	48
"	P	0.5	2.7×10^5	-24.0	0.0, -1.6	52
			VACHERIE dome			
885	P	0.5	7.8×10^6	-24.6	+1.6, +0.9	111,110
"	P	0.2	3.9×10^6	-33.1	+0.7, +0.6	70,71
1067.7	P	0.6	4.3×10^6	-22.5	+2.1, +1.6	109,110
"	S	3	--	-22.2	-1.3, -1.7	--
1432.5	P?	1.0	6.5×10^6	-25.1	-1.9, +1.3	92,93
"	P?	2.0	3.2×10^6	-25.2	+1.9, +1.6, +2.0	89,89
3222.5	P	0.5	1.4×10^6	-21.2	+1.9, +1.3	57,58
"	S?	2.5	7.7×10^4	-21.1	+2.1, +1.6	81,82

1/ P = primary, S = secondary

2/ The results of first and second runs are indicated for some; other, poorer inclusions in some of these samples yielded corroborative data.

3/ Cannot be determined, due to necking down.

4/ Inclusion leaked at 96°

5/ Volumes measured at room temperature after homogenization runs.

REFERENCES

Adams, L.H., and Gibson, R.E., 1930, The melting curve of sodium chloride dihydrate. An experimental study of an incongruent melting at pressures up to twelve thousand atmospheres: Jour Am. Chem. Soc., v. 52, p. 4252-4264.

Poty, Bernard, Leroy, Jacques, and Jachimowicz, Leon, 1976, A new device for measuring temperatures under the microscope: The Chaixmeca microthermometry apparatus: Bull. Soc. fr. Minéral. Cristallog., v. 99, p. 182-186 (in French; translated in Fluid Inclusion Research--Proceedings of COFFI, v. 9, 1976, p. 173-178.)

Roedder, Edwin, 1962, Studies of fluid inclusions I: Low-temperature application of a dual-purpose freezing and heating stage: Econ. Geology, v. 57, p. 1045-1061.

Roedder, Edwin, 1963, Studies of fluid inclusions II: Freezing data and their interpretation: Econ. Geology, v. 58, p. 167-211.

Roedder, Edwin, 1967, Metastable "superheated" ice in liquid-water inclusions under high negative pressure: Science, v. 155, p. 1413-1417.

Roedder, Edwin, 1970, Application of an improved crushing microscope stage to studies of the gases in fluid inclusions: Schweizer. Mineralog. u. Petrog. Mitt., v. 50, pt. 1, p. 41-58 (in English).

Roedder, Edwin, 1972, The composition of fluid inclusions. In Data of Geochemistry, Sixth Edition, M. Fleischer, Ed., U. S. Geological Survey Professional Paper 440JJ, 164 pp.

Roedder, Edwin, 1976, Fluid-inclusion evidence on the genesis of ores in sedimentary and volcanic rocks, Chapter 4 in Handbook of Strata-Bound and Stratiform Ore Deposits, ed. K.H. Wolf, Vol. 2, Geochemical Studies: Amsterdam, Elsevier Sci. Pub. Co., p. 67-110.

Roedder, Edwin, and Belkin, H.E., 1979a, Application of studies of fluid inclusions in Permian Salado Salt, New Mexico, to problems of siting the Waste Isolation Pilot Plant, in Scientific Basis for Nuclear Waste Management, vol. 1, G.J. McCarthy, ed.: New York, Plenum Press, p. 313-321.

Roedder, Edwin, and Belkin, H.E., 1979b, Migration of fluid inclusions in WIPP salt in thermal gradients: accepted for presentation at Second Materials Research Society Symposium on Scientific Basis for Nuclear Waste Management, Boston, Nov., 1979.